Journal of Neuroscience Research 65:129–138 (2001)

Effect of Osmotic Stress on Potassium Accumulation Around Glial Cells and Extracellular Space Volume in Rat Spinal Cord Slices

Lýdia Vargová,[1–3] Alexandr Chvátal,[1–3]* Miroslava Anděrová,[1–3] Šárka Kubinová,[1,2] Drahomír Žiak,[1] and Eva Syková[1–3]

[1]Department of Neuroscience, Institute of Experimental Medicine, Academy of Sciences of the Czech Republic, Prague, Czech Republic
[2]Department of Neuroscience, Charles University, Second Medical Faculty, Prague, Czech Republic
[3]Center for Cell Therapy and Tissue Repair, Charles University, Prague, Czech Republic

In rat brain and spinal cord slices, the local extracellular accumulation of K^+, as indicated by K^+ tail currents (I_{tail}) after a depolarization step, is greater in the vicinity of oligodendrocytes than that of astrocytes. It has been suggested that this may reflect a smaller extracellular space (ECS) around oligodendrocytes compared to astrocytes [Chvátal et al. [1997] J. Neurosci. Res. 49:98–106; [1999] J. Neurosci. Res. 56:493–505). We therefore compared the effect of osmotic stress in spinal cord slices from 5–11-day-old rats on the changes in reversal potentials (V_{rev}) of I_{tail} measured by the whole-cell patch-clamp technique and the changes in ECS volume measured by the real-time iontophoretic method. Cell swelling induced by a 20 min perfusion of hypoosmotic solution (200 mmol/kg) decreased the ECS volume fraction from 0.21 ± 0.01 to 0.15 ± 0.02, i.e., by 29%. As calculated from V_{rev} of I_{tail} using the Nernst equation, a depolarizing prepulse increased $[K^+]_e$ around astrocytes from 11.0 to 44.7 mM, i.e., by 306%, and around oligodendrocytes from 26.1 to 54.9 mM, i.e., by 110%. The ECS volume fraction decrease had the same time course as the changes in V_{rev} of I_{tail}. Cell shrinkage in hyperosmotic solution (400 mmol/kg) increased ECS volume fraction from 0.24 ± 0.02 to 0.32 ± 0.02, i.e., by 33%. It had no effect on $[K^+]_e$ evoked by a depolarizing prepulse in astrocytes, whereas in oligodendrocytes $[K^+]_e$ rapidly decreased from 52 to 26 mM, i.e., by 50%. The increase in ECS volume was slower than the changes in $[K^+]_e$. These data demonstrate that hypoosmotic solution has a larger effect on the ECS volume around astrocytes than around oligodendrocytes and that hyperosmotic solution affects the ECS volume around oligodendrocytes only. This indicates that increased K^+ accumulation in the vicinity of oligodendrocytes could be due to a restricted ECS. Oligodendrocytes in the CNS are therefore most likely surrounded by clusters of "compacted" ECS, which may selectively affect the diffusion of neuroactive substances in specific areas and directions and facilitate spatial K^+ buffering. J. Neurosci. Res. 65: 129–138, 2001. © 2001 Wiley-Liss, Inc.

Key words: astrocytes; diffusion; ECS volume fraction; extracellular space; hyperosmotic solution; hypoosmotic solution; oligodendrocytes; potassium tail currents

INTRODUCTION

The electrophysiological and morphological properties of rat spinal cord glial cells in the gray matter in situ have been examined in a number of studies (Chvátal et al., 1995, 1999; Pastor et al., 1995, 1998; Žiak et al., 1998). These studies revealed that mature astrocytes and oligodendrocytes express passive K^+ conductance during depolarization and hyperpolarization of the glial membrane. In contrast to the case in astrocytes, K^+ passive currents evoked in oligodendrocytes by a depolarizing or hyperpolarizing pulse decay, and large tail currents appear after the offset of the voltage jump. An analysis of the properties of oligodendrocyte tail currents in white as well as in gray matter revealed that they represent a rapid shift in K^+ caused by a change in the K^+ gradient across the cell membrane during the voltage step (Berger et al., 1991; Chvátal et al., 1999), so it was suggested that the large tail currents result from a more "compact" extracellular space (ECS) around oligodendrocytes than around astrocytes.

Extrasynaptic communication ("volume" transmission) between neurons and between neurons and glia is affected by the properties of the ECS: its structure and volume (for reviews see Fuxe and Agnati, 1991; Nicholson and Syková, 1998; Zoli et al., 1999; Syková and Chvátal, 2000). Changes

Contract grant sponsor: Grant Agency of the Czech Republic; Contract grant number: 305/99/0655; Contract grant number: 309/99/0657; Contract grant sponsor: Czech Ministry of Education, Youth and Sports; Contract grant number: VS 96 130; Contract grant number: LN00A065.

*Correspondence to: Alexandr Chvátal, PhD, Department of Neuroscience, Institute of Experimental Medicine, ASCR, Vídeňská 1083, 142 20 Praha 4, Czech Republic. E-mail: chvatal@biomed.cas.cz

Received 20 November 2000; Revised 26 February 2001; Accepted 27 February 2001

in the ECS diffusion parameters alter the diffusion of ions, transmitters, and other neuroactive substances in the CNS and may thus affect extrasynaptic transmission in the nervous tissue. The importance of the changes in ECS diffusion parameters increases during pathological states, when the concentration of toxic metabolites rapidly increases because of cell swelling and may cause serious injury to the neural cells (Syková, 1997; Syková et al., 2000).

Diffusion in the brain ECS is hindered by the size of the extracellular clefts; by the presence of membranes, fine neuronal and glial processes, macromolecules of the extracellular matrix (ECM), and charged molecules; and by cellular uptake. A mathematical description of diffusion in nervous tissue is possible only when Fick's original diffusion equations, describing diffusion in a free medium, are extended with the addition of three parameters (Nicholson and Phillips, 1981; Nicholson and Syková, 1998). First, diffusion in the CNS is constrained by the restricted volume of the tissue available for the diffusing molecules, i.e., by the ECS volume fraction (α) defined as the ratio between the volume of the ECS and the total volume of the tissue. Second, the free diffusion coefficient (D) of any substance in the brain is reduced by the tortuosity factor (λ) defined as $\lambda = (D/ADC)^{0.5}$, where D is the free diffusion coefficient of the substance and ADC is the apparent diffusion coefficient in the brain. The movement of any substance diffusing in the ECS is affected by membrane obstructions, macromolecules of the ECM, and cell processes. Third, substances released into the ECS are transported across membranes by specific, i.e., ATP-based, and nonspecific uptake. In experiments in which the real-time TMA^+ iontophoretic method using TMA^+-sensitive microelectrodes is used to measure the absolute values of volume fraction and tortuosity and to determine the time course of their changes in nervous tissue (Nicholson and Philips, 1981; Nicholson and Syková, 1998), nonspecific uptake of TMA^+ is characterized by a kinetic constant, k' (sec^{-1}). Using the real-time iontophoretic method, ECS diffusion parameters are, however, averaged over a volume on the order of 10^{-3} mm^3; therefore, this method provides no information about changes in the diffusion parameters in the closer vicinity of individual nerve cells.

In the present study, we analyzed the effect of hyper- and hypoosmotic solutions on astrocyte and oligodendrocyte tail currents in the dorsal horn of the rat spinal cord slice. Tail current analysis was used in the present study for the estimation of $[K^+]_e$ changes in the ECS in the vicinity of the cell membranes evoked by the osmotic stress. The time course of the observed changes in tail currents was correlated with the changes in the extracellular space diffusion parameters (ECS volume fraction and tortuosity), as measured by the real-time iontophoretic TMA^+ method.

MATERIALS AND METHODS

Preparation of Spinal Cord Slices and Electrophysiological Setup

Spinal cord slices were prepared as described previously (Chvátal et al., 1995). In brief, rats were sacrificed while under ether anesthesia at postnatal days 8–10 (P8–10) by decapitation. The spinal cords were quickly dissected out and washed in artificial cerebrospinal fluid (ACF) at 8–10°C. A 4–5-mm-long segment of the lumbar cord was embedded in 1.7% agar at 37°C (Purified Agar; Oxoid Ltd.). Transverse 200- or 400-μm-thick slices were made using a vibroslice (752M; Campden Instruments). Slices were individually transferred to a recording chamber mounted on the stage of a Zeiss fluorescence microscope (Axioskop FX) and fixed using a U-shaped platinum wire with a grid of nylon threads (Edwards et al., 1989). The chamber was continuously perfused with oxygenated ACF. All experiments were carried out at room temperature (~22°C).

Solutions

The ACF contained (in mM): NaCl 117.0, KCl 3.0, $CaCl_2$ 1.5, $MgCl_2$ 1.3, Na_2HPO_4 1.25, $NaHCO_3$ 35.0, and D-glucose 10.0 (osmolality 300 mmol/kg). The solution was continuously gassed with a mixture of 95% O_2 and 5% CO_2 to maintain a final pH of 7.4. Hypoosmotic solution (200 mmol/kg) contained 69.0 mM NaCl instead of 117 mM; hyperosmotic solution (400 mmol/kg), in addition to isotonic ACF, contained 87.6 mM sucrose. Osmolality was measured using a vapor pressure osmometer (Vapro 5520; Wescor Inc., Logan, UT). The perfusion rate of the ACF in the recording chamber (~2 ml volume) was 5 ml/min.

Patch-Clamp Recordings

Cell somata in the spinal cord slice were approached by the patch electrode (Fig. 1A) using an Infrapatch system (Luigs and Neumann, Ratingen, Germany). The cells in the slice and the recording electrode were imaged with an infrared-sensitive video camera (C2400-03; Hamamatsu Photonics, Hamamatsu City, Japan) and displayed on a standard TV/video monitor. Selected cells with a membrane potential more negative than –50 mV had a clear, dark membrane surface and were located 5–10 μm below the slice surface. Membrane currents were measured with the patch-clamp technique in the whole-cell recording configuration (Hamill et al., 1981). Current signals were amplified with an EPC-9 amplifier (HEKA Elektronik, Lambrecht/Pfalz, Germany), filtered at 3 kHz and sampled at 5 kHz by an interface connected to an AT-compatible computer system, which also served as a stimulus generator.

Recording pipettes for patch-clamp recordings were pulled from borosilicate capillaries (Kavalier, Otvovice, Czech Republic) using a Brown-Flaming micropipette puller (P-97; Sutter Instruments Company) with a tip resistance of 4–6 MΩ. The internal pipette solution had the following composition (in mM): KCl 130.0, $CaCl_2$ 0.5, $MgCl_2$ 2.0, EGTA 5.0, HEPES 10.0. The pH was adjusted with KOH to 7.2.

Diffusion Measurements

Changes in ECS diffusion parameters were studied by means of the real-time iontophoretic TMA^+ method (Syková et al., 1999; Fig. 1E–G). In brief, a substance to which cell membranes are relatively impermeable, i.e., tetramethylammonium (TMA^+), was administered into the ECS of the spinal cord slice using an iontophoretic microelectrode, made from theta glass tubing (Clark Electromedical Instruments) and filled with 100 mM TMA^+. The concentration of TMA^+ was measured at

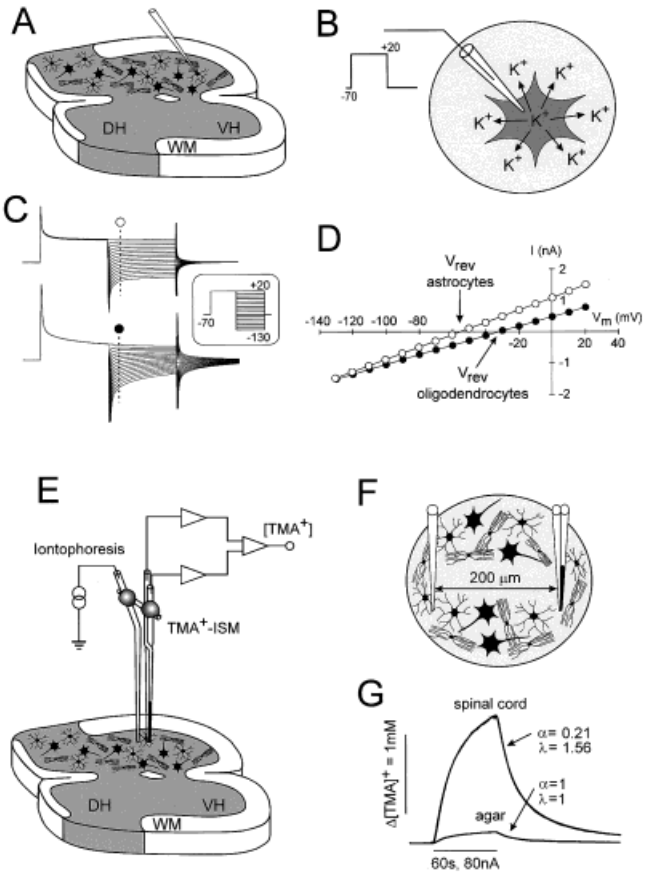

Fig. 1. Experimental setup for the tail current analysis (**A–D**) and the TMA^+ real-time iontophoretic method (**E–G**). Membrane currents of astrocytes and oligodendrocytes were recorded in the dorsal horn area of the gray matter of the spinal cord slice during and after a depolarizing pulse (A). Because the membrane of glial cells is almost perfectly permeable to K^+, such a depolarization causes an efflux of K^+ from the cell (B). For the tail current analysis, the membranes of astrocytes (open circles) and oligodendrocytes (solid circles) were clamped from a holding potential of −70 mV to +20 mV for 20 msec (C). After this prepulse, the membrane was clamped for 20 msec to increasing de- and hyperpolarizing potentials (pattern of voltage commands in **inset**) ranging from −130 mV to +20 mV, at 10 mV increments. From traces as shown in C, which represents recordings from a typical astrocyte and a typical oligodendrocyte, currents (I) were measured 5 msec after the onset of the de- and hyperpolarizing pulses (dashed lines) and plotted as a function of the membrane potential (V_m; D). The reversal potentials (V_{rev}) determined for the astrocyte and oligodendrocyte shown in C are indicated in the graphs by the arrows. Tetramethylammonium (TMA^+) was administered into the nervous tissue using an iontophoretic electrode (E). The concentration of TMA^+ was then measured in the ECS by means of a double-barreled TMA^+-sensitive microelectrode (ISM). TMA^+-ISM and iontophoretic electrodes were glued together and lowered into the gray matter of the spinal cord slice with an intertip distance of 160–200 µm (F). The diffusion curves obtained from the spinal cord slices were analyzed by fitting the data to a solution of the modified diffusion equation to yield the diffusion parameters of the spinal cord nervous tissue, namely, volume fraction α and tortuosity λ (G). The microelectrode array was first calibrated in agar, where $\alpha = 1 = \lambda$, and then the values of α and λ were obtained in the spinal cord slice.

a given distance of 160–200 µm (Fig. 1F) using a double-barreled TMA^+-ion sensitive microelectrode (TMA^+-ISM). ISMs for TMA^+ were prepared as previously described (for details see Syková et al., 1994). The ion exchanger was Corning 477317 and the TMA^+-sensitive barrel was back-filled with 100 mM TMA^+ chloride. The reference barrel contained 150 mM NaCl. Electrodes were calibrated using the fixed-interference method before and after each experiment in a sequence of flowing solutions containing 0.01, 0.03, 0.1, 0.3, 1.0, 3.0, and 10.0 mM TMA^+ in a background of 150 mM NaCl. Calibration data were fitted with the Nikolsky equation to determine electrode slope and interference (Nicholson and Philips, 1981). The shank of the iontophoretic electrode was bent so that it could be aligned parallel to that of the ISM (Fig. 1E). Both TMA^+-ISM and iontophoretic electrodes were glued together with dental cement, and the intertip distance was adjusted to 160–200 µm. To calibrate the microelectrode array, TMA^+ diffusion curves were first recorded in 0.3% agar (Special Noble Agar; Difco, Detroit, MI) made up in 150 mM NaCl, 3 mM KCl, and 1 mM TMACl (Fig. 1G). Typical parameters for the iontophoretic application of TMA^+ were: bias current +20 nA (to keep a constant transport number of the iontophoretic electrode) and current step +80 nA for 60 sec. The microelectrode array was then lowered into the 400-µm-thick spinal cord slice to a depth of about 200 µm. The diffusion curves obtained from the spinal cord slices were transferred to a PC-based computer and analyzed by fitting the data to a solution of the modified diffusion equation using Voltoro software (Nicholson, unpublished) to yield the diffusion parameters of the spinal cord nervous tissue, namely, volume fraction α and tortuosity λ (Fig. 1G).

Intracellular Staining of Cells

During electrophysiological recording, selected cells were filled with Lucifer yellow (LY) by dialyzing the cytoplasm with a patch pipette solution containing 1 mg/ml LY dilithium salt (Sigma, St. Louis, MO). To avoid destruction of the cell by removing the pipette after the recording, we destroyed the seal by injection of a large hyperpolarizing current. The morphology of LY-filled cells was examined in unfixed slices in situ after electrophysiological recordings using a fluorescence microscope equipped with a fluorescein isothiocyanate filter combination (band pass 450–490 nm, mirror 510 nm, long pass 520 nm).

RESULTS

Electrophysiological and Morphological Identification of Astrocytes and Oligodendrocytes

Patch-clamp recordings were performed on glial cells in the dorsal horn gray matter of rat spinal cord slices from animals 8–10 days old (P8–10). This postnatal period is characterized by gliogenesis; it was shown in our previous study, in which glial precursor cells and mature glial cells were identified electrophysiologically and immunohistochemically (Chvátal et al., 1995), that the number of glial precursors decreases during the period from P4 to P18, while the number of mature astrocytes and oligodendrocytes increases. Mature astrocytes and oligodendrocytes in the present study were identified on the basis of our

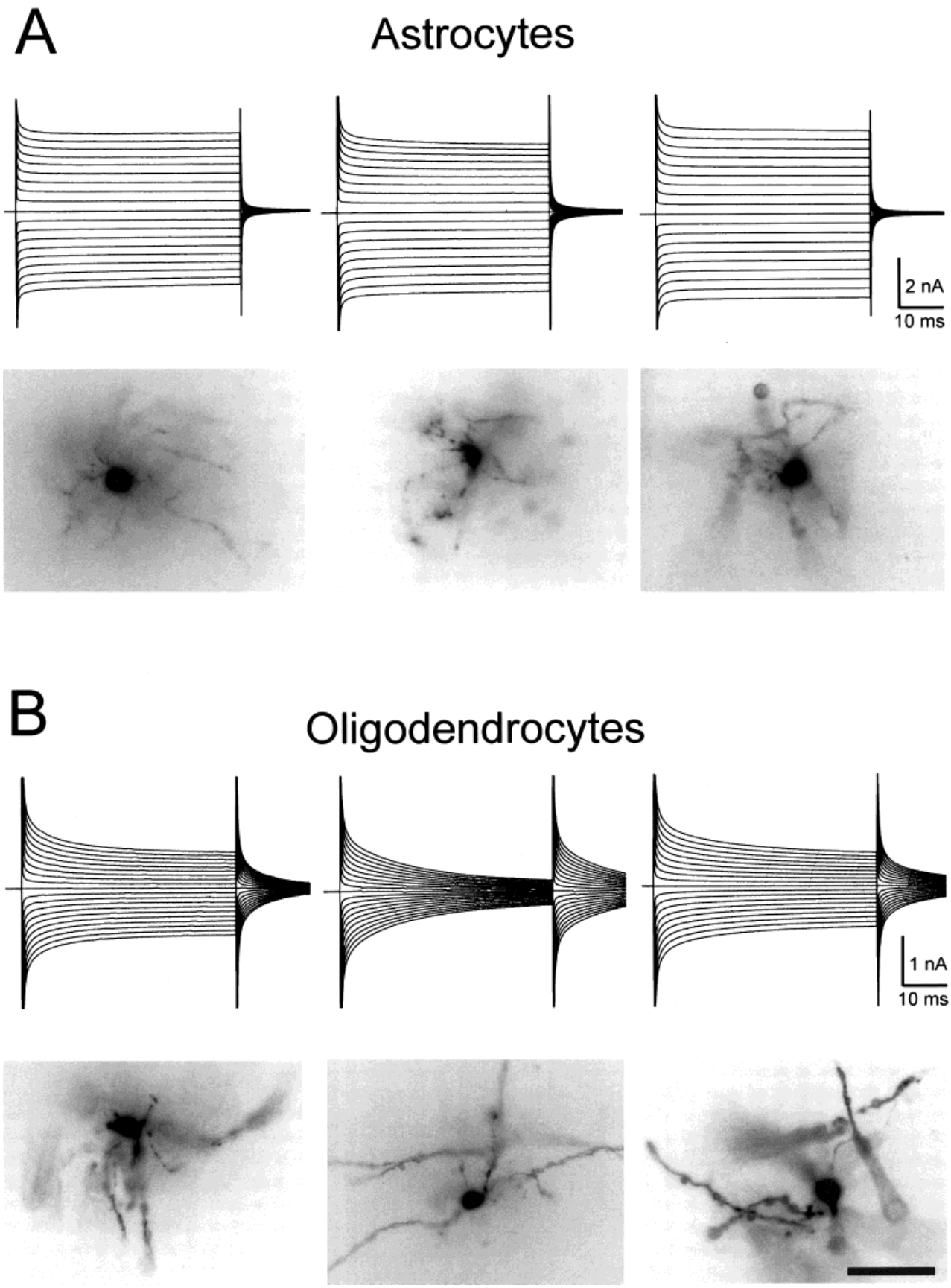

Fig. 2. Membrane currents and respective photomicrographs of three typical astrocytes (**A**) and oligodendrocytes (**B**). Membrane currents were recorded in response to voltage steps from a holding potential of −70 mV. To activate the currents, the membrane was clamped for 50 msec to increasing de- and hyperpolarizing potentials ranging from −160 to +20 mV, at 10 mV increments. The corresponding current traces are superimposed. During recording, cells were filled with Lucifer yellow by dialyzing the cytoplasm with the patch pipette solution. After recording, the morphology of Lucifer yellow-filled cells was examined with a fluorescence microscope.

previous electrophysiological, morphological, and immunohistochemical analysis of glial cells in rat spinal cord slices (Chvátal et al., 1995; Pastor et al., 1995).

The current patterns observed after clamping the glial cell membrane from the holding potential of –70 mV to values ranging from –160 mV to +20 mV clearly distinguished between astrocytes and oligodendrocytes. Astrocytes were characterized by large, symmetrical, non-decaying K^+-selective currents during the voltage jump (Fig. 2A), whereas oligodendrocytes were characterized by symmetrical, passive but decaying K^+ currents (Fig. 2B). After the offset of the depolarizing or hyperpolarizing voltage step, large symmetrical inward and outward tail currents (I_{tail}) appeared in oligodendrocytes. Such tail currents were not observed in astrocytes. Electrophysiologically identified astrocytes and oligodendrocytes were filled with LY, and their morphology was examined (Fig. 2A,B). Most astrocytes, which were characterized by round cell bodies 8–10 μm in diameter, were surrounded by very fine processes that formed a diffuse network (Fig. 2A). The values for the somatic diameter were measured using infrared optics, because the LY fluorescence image, shown in Figure 2, gives the impression of a larger somatic diameter as a result of the high fluorescence of the soma in comparison to the processes, which leads to film overexposure (see also Chvátal et al., 1995). Oligodendrocytes had a round cell body about 10–15 μm in diameter, and, in contrast to astrocytes, the majority of cells displayed long and often parallel processes (Fig. 2B).

Effect of Hyper- and Hypoosmotic Stress on K^+ Accumulation After a Depolarizing Prepulse

K^+ tail currents were analyzed from measurements performed during a series of 20 msec test pulses from –130 mV to +20 mV following a depolarizing voltage step of 90 mV, i.e., by changing the holding potential from –70 mV to +20 mV for 20 msec (Fig. 1B,C; Chvátal et al., 1999). The reversal potential (V_{rev}) of the glial membrane after the depolarizing prepulse was determined from the current/voltage (I/V) relationship measured 5 msec after the onset of the de- and hyperpolarizing pulses (Fig. 1D). The values of glial cell membrane potential (V_m) were determined by switching the EPC-9 amplifier to the current-clamp mode. V_{rev} and V_m were measured every 3 min before, during, and after the application of hyper- or hypoosmotic solution (Figs. 3, 4). Under resting conditions, V_{rev} shifted to more positive values in oligodendrocytes than in astrocytes, even when comparable outward currents were evoked at the beginning of the pulse. V_{rev} was –27.6 ± 4.0 mV (mean ± SEM, n = 10) in oligodendrocytes and –53.9 ± 2.2 mV (n = 10) in astrocytes.

Cell swelling evoked by the application of hypoosmotic solution for 20 min, i.e., by changing the osmolality of the ACF from 300 to 200 mmol/kg, had a greater effect on V_{rev} in astrocytes than in oligodendrocytes (Fig. 3). In astrocytes, V_{rev} increased from –50.4 ± 2.4 to –26.1 ± 6.0 mV (n = 5); in oligodendrocytes, it increased from –35.4 ± 3.2 to –20.7 ± 6.0 mV (n = 5). During the application of hypoosmotic solution, V_m shifted to more negative values by 2–3 mV in both astrocytes and oligodendrocytes. Because the glial membrane is exclusively permeable to K^+, the Nernst equation was used to calculate the extracellular K^+ concentration ($[K^+]_e$) in the vicinity of the cell membrane from the values of V_m and V_{rev} (Chvátal et al., 1997, 1999). $[K^+]_e$ calculated from the values of V_m did not significantly change during the application of hypoosmotic solution in either astrocytes or oligodendrocytes, whereas $[K^+]_e$ calculated from the values of V_{rev} increased in astrocytes from 17.9 ± 1.6 to 50.9 ± 14.3 mM and in oligodendrocytes from 32.8 ± 4.0 to 61.4 ± 11.1 mM.

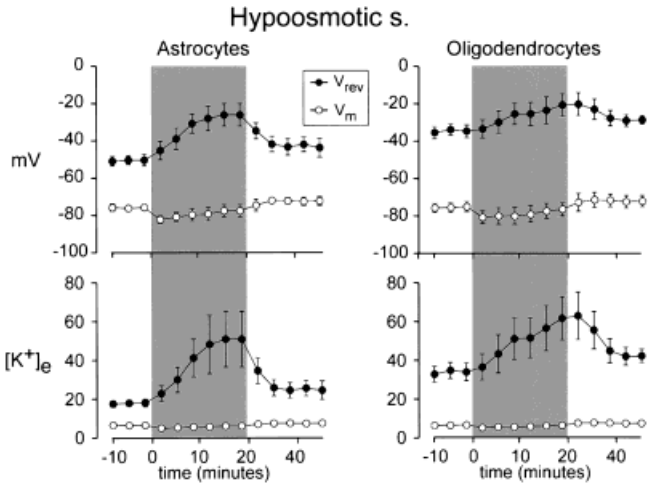

Fig. 3. Effect of hypoosmotic solution on membrane potential (V_m) and reversal potential (V_{rev}) of tail currents in astrocytes and oligodendrocytes. Application of hypoosmotic solution (200 mmol/kg) evoked in both astrocytes and oligodendrocytes a shift of V_m to more negative values and a shift of V_{rev} of the tail currents to more positive values. The Nernst equation was used to calculate the corresponding extracellular K^+ concentration ($[K^+]_e$) from the values of V_m and V_{rev} of the tail currents.

Cell shrinkage evoked by the application of hyperosmotic solution (400 mmol/kg) had different effects on V_{rev} in oligodendrocytes and in astrocytes (Fig. 4). There was no significant effect of hyperosmotic solution on astrocytes, whereas in oligodendrocytes V_{rev} decreased from –20.3 ± 5.0 mV (n = 5) in normal to –32.0 ± 2.2 mV in hyperosmotic solution. In contrast to the case in hypoosmotic solution, V_m did not significantly change during the application of hyperosmotic solution in either astrocytes or oligodendrocytes. $[K^+]_e$ calculated from the mean values of V_{rev} decreased in oligodendrocytes from 61.9 ± 12.5 to 37.0 ± 3.2 mM.

Cell Volume Changes and ECS Diffusion Parameters

Osmotic stress results in swelling or shrinkage of cells, particularly glia. Diffusion measurements revealed that the same osmotic stress as was used in patch-clamp recordings leads to dramatic changes in ECS volume fraction (Figs. 5, 6). A 20 min superfusion of the spinal cord slice with hypoosmotic solution (200 mmol/kg) evoked a

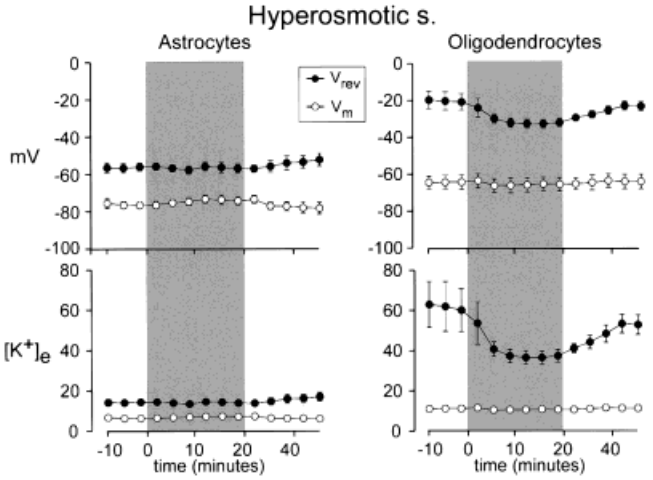

Fig. 4. Effect of hyperosmotic solution on membrane potential and reversal potential of tail currents in astrocytes and oligodendrocytes. Application of hyperosmotic solution (400 mmol/kg) had no effect on membrane potentials (V_m) or on reversal potentials (V_{rev}) of the tail currents in astrocytes. In oligodendrocytes, V_{rev} of the tail currents shifted to more negative values. The extracellular K^+ concentration ($[K^+]_e$) evoked by depolarizing pulses decreased around oligodendrocytes in hyperosmotic solution.

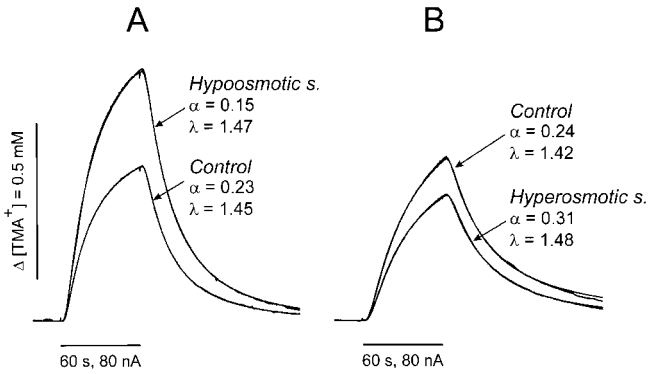

Fig. 5. Tetramethylammonium diffusion curves during the application of hypoosmotic and hyperosmotic solutions. Typical tetramethylammonium (TMA^+) diffusion curves recorded in isotonic solution (Control) and during the application of hypoosmotic (**A**) and hyperosmotic (**B**) solutions. The corresponding values of α and λ calculated from the diffusion curves are indicated with each diffusion curve.

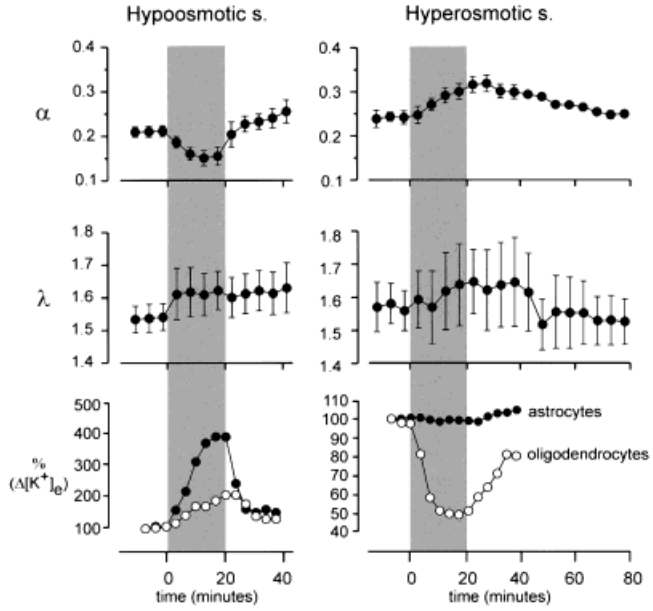

Fig. 6. Time course of the changes in diffusion parameters and in extracellular potassium during the application of hypoosmotic and hyperosmotic solutions. From the values obtained from the diffusion curves shown in Figure 5, graphs were constructed showing the time course of the changes in α and λ before, during, and after the application of hypo- and hyperosmotic solutions. The changes in the net increase of K^+ ($\Delta[K^+]_e$, calculated from the values of $[K^+]_e$ derived from V_m and V_{rev} of I_{tail}) are represented as percentage of control values of $\Delta[K^+]_e$. In both astrocytes and oligodendrocytes, the application of hypoosmotic solution evoked an increase in $\Delta[K^+]_e$. A similar time course was observed in the changes of the extracellular volume fraction α. The application of hyperosmotic solution, however, evoked a decrease in $\Delta[K^+]_e$ in oligodendrocytes only, and this decrease had a faster time course than the changes in the volume fraction α.

reversible decrease in α from 0.21 ± 0.01 to 0.15 ± 0.02 (n = 5). The decrease in α was accompanied by an increase in λ from 1.54 ± 0.04 to 1.62 ± 0.06. A 20 min application of hyperosmotic solution (400 mmol/kg) led to an increase in α from 0.24 ± 0.01 to 0.30 ± 0.02 (n = 5). No significant changes in λ were observed during superfusion of the spinal cord slice with hyperosmotic solution (see also Syková et al., 1999). The changes in α evoked by hypoosmotic solution occurred significantly more quickly than those evoked by hyperosmotic solution; the maximal changes were observed at about 10–15 min and at 15–20 min, respectively. The recoveries to control values took 20 and 60 min, respectively (Fig. 6).

The time courses of changes in ECS diffusion parameters evoked by osmotic stress were compared to the changes in the net increase in $[K^+]_e$ ($\Delta[K^+]_e$) evoked by depolarizing pulses in astrocytes and oligodendrocytes. $\Delta[K^+]_e$ represents the difference between the values of $[K^+]_e$ calculated from V_m and from V_{rev} as shown in Figures 3 and 4. Around astrocytes, $\Delta[K^+]_e$ increased from 11.0 mM in normal to 44.7 mM in hypoosmotic solution, i.e., by 306% (Fig. 6). In oligodendrocytes, the net increase in $[K^+]_e$ was much smaller: It rose from 26.1 mM in normal to 54.9 mM in hypoosmotic solution, i.e., by 110%. Hyperosmotic solution had no effect on $\Delta[K^+]_e$ evoked by depolarizing pulses in astrocytes, whereas, in oligodendrocytes, $\Delta[K^+]_e$ decreased from 52.4 to 26 mM, i.e., by 50% (Fig. 6).

DISCUSSION

Oligodendrocyte Tail Currents In Situ Are Determined by the Properties of the Nervous Tissue

The first electrophysiological studies performed on glial cells from the *Necturus* optic nerve revealed that the

glial membrane is almost exclusively permeable to K^+ (Kuffler et al., 1966). In addition, our previous experiments performed on glial cells in situ have shown that superfusion of rat spinal cord slices with 55 mM K^+ shifts the reversal potential of astrocytes, oligodendrocytes, and glial precursor cells to –16 mV, which is close to the estimated equilibrium potential (–23 mV) as calculated from the Nernst equation (Chvátal et al., 1995). The glial membrane potential is thus strictly dependent on the distribution of K^+ inside and outside the cell. An increase in $[K^+]_e$ depolarizes the cell and shifts the V_{rev} of the membrane to positive values. Depolarization of the glial cell produces an efflux of K^+ across the cell membrane and its accumulation in the vicinity of the cell. Potassium accumulation is dependent on the pore size around cells and is accompanied by a decrease in current during the voltage step as well as by the presence of tail currents (Chvátal et al., 1999; Chvátal and Syková, 2000). Studies performed on astrocytes and oligodendrocytes in culture, where the extracellular space is infinite, did not reveal either a current decay during the depolarizing step or the presence of tail currents or shifts of V_{rev} (Sontheimer et al., 1989; Glassmeier et al., 1992). However, measurements performed in brain slices, i.e., in tissue with a preserved extracellular microenvironment, revealed a current decay during the depolarizing pulse and the presence of large tail currents in oligodendrocytes or oligodendrocyte-like cells, but not in astrocytes or glial precursor cells (Berger et al., 1991; Steinhäuser et al., 1992; Chvátal et al., 1997, 1999; Hinterkeuser et al., 2000). Such distinct membrane properties of oligodendrocytes are therefore determined by the properties of the intact nervous tissue, i.e., by the presence of different types of cellular elements, cell processes, molecules of the extracellular matrix, and a small ECS volume.

K^+ Accumulation Around Oligodendrocytes Results From a Compact ECS Volume

It was suggested that the large shift of V_{rev} in oligodendrocytes after the voltage step is produced by a larger K^+ accumulation in the more "compact" ECS around oligodendrocyte membranes (Chvátal et al., 1999). Because the membrane of astrocytes and oligodendrocytes is nearly perfectly permeable for K^+, the Nernst equation was used in our previous studies (Chvátal et. al., 1997, 1999) as well as in the current study to calculate $[K^+]$ in the vicinity of the glial membrane. There are certain limitations in the accuracy of the calculated $[K^+]$, because we did not consider the permeability of the membrane to other ions, potassium gradients inside the cells, or changes in intracellular $[K^+]$, which may take place even when the intracellular composition is controlled by the patch pipette (see also Chvátal et al., 1999). However, all the above-mentioned factors would similarly affect the accuracy of measurements in all types of glial cells and thus cannot be responsible for the observed $[K^+]$ differences in the vicinity of astrocytes and oligodendrocytes.

The findings that the V_{rev} of the oligodendrocyte membrane in situ is dependent on the duration and amplitude of the preceding voltage step (Berger et al., 1991; Steinhäuser et al., 1992; Chvátal et al., 1997, 1999) and that tail currents are abolished by the application of Ba^{2+}, a K^+ channel blocker (Chvátal et al., 1995), support a potassium origin of the oligodendrocyte tail current (for review see Chvátal and Syková, 2000). Our previous study found a correlation between an increasing number of oligodendrocytes in the white matter during early postnatal development and both a shift in V_{rev} to more positive values and a decrease in the ECS volume fraction (Chvátal et al., 1997). However, morphological investigation of astrocytes and oligodendrocytes, using LY staining, did not reveal any link between a particular cell's displaying either current decay or tail currents and that cell's morphology. Even though the majority of oligodendrocytes display long, parallel processes (see Fig. 1), such a morphological difference cannot be responsible for the nearly tenfold difference in K^+ accumulation in the vicinity of the oligodendrocyte membrane evoked by the depolarizing pulse. It is, therefore, possible to assume that the greater K^+ accumulation in the vicinity of oligodendrocytes occurs in the narrow intercellular clefts between oligodendrocyte processes and enwrapped axons; however, further ultrastructural investigation is needed to answer this question.

Changes in Oligodendrocyte Tail Currents Coincide With Changes in ECS Volume

The application of hypoosmotic or hyperosmotic solutions evokes complex effects in neural cells: It affects cell size as well as the metabolic and membrane properties of glial cells. The majority of osmotic studies to date have been performed on cell cultures, and little information is available about the effect of osmotic stress on glial cells in acute brain slices or in vivo. Studies using morphological analysis, light scattering, flow cytometry, or fluorescence techniques performed on glial cells in culture have shown that a hypoosmotic solution produces swelling of the cells, whereas the application of a hyperosmotic solution results in cell shrinkage (Del Bigio et al., 1992; Eriksson et al., 1992; McManus and Strange, 1993; Tomita et al., 1994; Flögel et al., 1995). Diffusion-weighted ^{1}H-nuclear magnetic resonance (NMR) spectroscopy has shown that such cell volume changes are accompanied by pronounced changes in the content of a number of organic osmolytes. For example, Flögel et al. (1995) observed that adaptation of intra- to extracellular osmolarity is mediated by a decrease in the cytosolic taurine level under hypoosmotic stress and by an intracellular accumulation of amino acids under hyperosmotic stress.

In patch-clamp studies of cultured astrocytes and oligodendrocytes, an increase in membrane K^+ and Cl^- conductance evoked by hypoosmotic solution was observed (Kimelberg et al., 1990; Olson and Li, 1997). Changes in conductance were, however, similar in astrocytes and oligodendrocytes. In our experiments, hypoosmotic solution evoked a larger effect in astrocytes than in oligodendrocytes, suggesting that differences in V_{rev} of I_{tail} in astrocytes and in oligodendrocytes are not caused by changes in membrane conductance, local intracellular pH

changes, or modulation of voltage-activated K^+ channels but rather by differences in the ECS volume in the vicinity of individual glial cells. Our conclusion is also supported by the effect of hyperosmotic solution, which affected V_{rev} of I_{tail} in oligodendrocytes only. In studies performed in cultured glial cells, the application of hyper- or hypoosmotic solutions evoked changes in the glial membrane potential on the order of 5–10 mV (Kimelberg and O'Connor, 1988; Kimelberg and Kettenmann, 1990). In our experiments, the application of hypoosmotic solution evoked a hyperpolarization of astrocytes and oligodendrocytes by 2–3 mV, whereas the application of hyperosmotic solution had no effect on glial membrane potential. Insofar as cell volume regulation involves a number of distinct ionic channels, transporters, and carriers, the observed differences may arise from the different membrane properties of glial cells in culture and in acute brain slices.

Changes of V_{rev} in glial cells after a depolarizing pulse most likely result from K^+ accumulation in the restricted ECS volume; we found, during osmotic stress, concomitant changes in V_{rev} and in two ECS diffusion parameters, volume fraction and tortuosity. Hypoosmotic solution evoked a decrease in volume fraction, whereas hyperosmotic solution evoked an increase in volume fraction. Similar decreases in ECS volume fraction evoked by the application of hypoosmotic solution were observed in isolated turtle cerebellum (Krizaj et al., 1996), in isolated rat spinal cord (Syková et al., 1999), and in isolated frog spinal cord and filum terminale (Prokopová-Kubinová and Syková, 2000) and correspond to cell swelling. In contrast to others' experiments performed in cell cultures (Eriksson et al., 1992; Del Bigio et al., 1992; McManus and Strange, 1993; Flögel et al., 1995) or in the isolated spinal cord (Syková et al., 1999), our experiments showed neither an initial swelling in hypoosmotic solution followed by a regulatory volume decrease (RVD) nor an initial period of shrinkage in hyperosmotic solution followed by a regulatory volume increase (RVI). There might be two explanations for this phenomenon. First, as suggested by Krizaj et al. (1996), there is a gradual exposure to the osmotic stress in the spinal cord slice in contrast to cultured cells, and, second, as shown in a study performed on isolated spinal cord (Syková et al., 1999), owing to incomplete gliogenesis, RVD is less effective in immature animals as were used in the present study.

Osmotic stress in our experiments did not evoke significant changes in ECS tortuosity. This is in agreement with previous studies performed in other brain slice preparations (Pérez-Pinzon et al., 1995; Krizaj et al., 1996). Syková et al. (1999) suggested that the tortuosity changes observed in mammalian brain slices may be artificially low, possibly because of the washing out of macromolecules from the ECS or reduced swelling of cut cellular processes. In contrast to the case in brain slices, long-term changes in tortuosity were revealed in the isolated rat spinal cord, most likely related to astrogliosis (Syková et al., 1999).

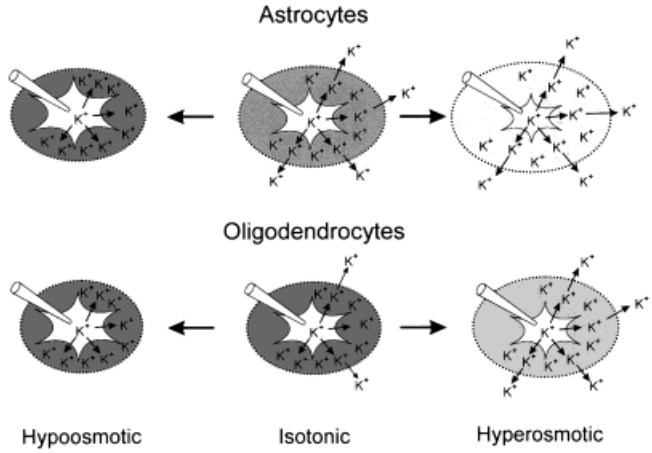

Fig. 7. A model of potassium flow across the membrane of oligodendrocytes and astrocytes as evoked by a depolarizing pulse in hypoosmotic and hyperosmotic solutions. Hypoosmotic solution produces swelling of astrocytes and oligodendrocytes, enhanced tail currents resulting from increased $[K^+]_e$, and a decrease in the size of the ECS. Hyperosmotic solution produces cell shrinkage, resulting in an increase of ECS volume fraction and in a decrease of tail currents in oligodendrocytes as a result of decreased K^+ accumulation. For further explanation, see text.

Oligodendrocyte Tail Currents Reveal Heterogeneity of the Gray Matter

Our results demonstrate that the time course of K^+ accumulation around glial membranes evoked by a depolarizing pulse is related to changes in the ECS volume fraction during osmotic stress (Fig. 6). We therefore propose a model of $[K^+]_e$ changes in the vicinity of astrocytes and oligodendrocytes evoked by a depolarizing pulse during the application of hypoosmotic and hyperosmotic solutions (Fig. 7). In isotonic ACF, where the ECS in the vicinity of the oligodendrocytes is more compact than that around astrocytes, a depolarizing pulse produces greater K^+ accumulation around oligodendrocytes. Hypoosmotic solution evokes swelling of astrocytes as well as oligodendrocytes. The decrease in ECS volume fraction in the vicinity of these cells represented by the increase in K^+ accumulation is, however, more pronounced around oligodendrocytes than around astrocytes because of the smaller initial ECS around oligodendrocytes. Conversely, the application of hyperosmotic solution evokes a shrinkage of glial cells as well as an increase in the ECS volume fraction in the vicinity of astrocytes and oligodendrocytes. Because there is a relatively large ECS around astrocytes in isotonic ACF, astrocyte shrinkage does not affect K^+ accumulation in response to a depolarizing pulse. In contrast, ECS volume in the vicinity of an oligodendrocyte substantially increases during oligodendrocyte shrinkage, producing a decrease in K^+ accumulation.

We conclude that differences in K^+ accumulation around glial cells evoked by membrane depolarization are affected by the heterogeneous ECS in the vicinity of cells. There is still no direct ultrastructural evidence for a "compacted" ECS around oligodendrocytes; however, preliminary data obtained using a mathematical model that describes K^+ accumulation in the vicinity of passive glial cells (Chvátal et al., 2000) support our hypothesis. The presence of perineuronal nets and the different compositions of the extracellular matrix around astrocytes, oligodendrocytes, and neurons (Margolis and Margolis, 1974; Brückner et al., 1996) may also contribute to the spatial heterogeneity of the ECS. Insofar as neuronal activity is accompanied by an increase in $[K^+]_e$ and by changes in $[Ca^{2+}]$, pH, and other ions in the ECS (Chvátal et al., 1988; Syková, 1992), we may speculate that heterogeneities in the nervous tissue, represented by "clusters" of compact ECS around oligodendrocytes, can facilitate K^+ spatial buffering in gray matter, as was suggested for oligodendrocytes in corpus callosum (Chvátal et al., 1997), and selectively affect the diffusion of ions and other neuroactive substances in specific areas and directions.

REFERENCES

Berger T, Schnitzer J, Kettenmann H. 1991. Developmental changes in the membrane current pattern, K^+ buffer capacity and morphology of glial cells in the corpus callosum slice. J Neurosci 11:3008–3024.

Brückner G, Bringmann A, Köppe G, Härtig W, Brauer K. 1996. In vivo and in vitro labeling of perineuronal nets in rat brain. Brain Res 720:84–92.

Chvátal A, Syková E. 2000. Glial influence on neuronal signaling. Progr Brain Res 125:199–216.

Chvátal A, Jendelová P, Kříž N, Syková E. 1988. Stimulation-evoked changes in extracellular pH, calcium and potassium activity in the frog spinal cord. Physiol Bohemoslov 37:203–212.

Chvátal A, Pastor A, Mauch M, Syková E, Kettenmann H. 1995. Distinct populations of identified glial cells in the developing rat spinal cord: ion channel properties and cell morphology. Eur J Neurosci 7:129–142.

Chvátal A, Berger T, Voříšek I, Orkand RK, Kettenmann H, Syková E. 1997. Changes in glial K^+ currents with decreased extracellular volume in developing rat white matter. J Neurosci Res 49:98–106.

Chvátal A, Anděrová M, Žiak D, Syková E. 1999. Glial depolarization evokes a larger potassium accumulation around oligodendrocytes than around astrocytes in gray matter of rat spinal cord slices. J Neurosci Res 56:493–505.

Chvátal A, Anděrová M, Syková E. 2000. A mathematical model of K^+ accumulation in the vicinity of astrocytes and oligodendrocytes in the rat spinal cord. Soc Neurosci Abstr 26:1899.

Del Bigio MR, Fedoroff S, Qualtiere LF. 1992. Morphology of astroglia in colony cultures following transient exposure to potassium ion, hypoösmolarity and vasopressin. J Neurocytol 21:7–18.

Edwards FA, Konnerth A, Sakmann B, Takahashi T. 1989. A thin slice preparation for patch clamp recordings from neurones of the mammalian central nervous system. Pflügers Arch 414:600–612.

Eriksson PS, Nilsson M, Wagberg M, Rönnbäck L, Hansson E. 1992. Volume regulation of single astroglial cells in primary culture. Neurosci Lett 143:195–199.

Flögel U, Niendorf T, Serkowa N, Brand A, Henke J, Leibfritz D. 1995. Changes in organic solutes, volume, energy state, and metabolism associated with osmotic stress in a glial cell line: a multinuclear NMR study. Neurochem Res 20:793–802.

Fuxe K, Agnati LF. 1991. Volume transmission in the brain: novel mechanisms for neural transmission. New York: Raven Press.

Glassmeier G, Jeserich G, Krüppel T. 1992. Voltage-dependent potassium currents in cultured trout oligodendrocytes. J Neurosci Res 32:301–308.

Hamill OP, Marty A, Neher E, Sakmann B, Sigworth FJ. 1981. Improved patch-clamp techniques for high-resolution current recording from cells and cell-free membrane patches. Pflügers Arch 391:85–100.

Hinterkeuser S, Schröder W, Hager G, Seifert G, Blümcke I, Elger CE, Schramm J, Steinhäuser C. 2000. Astrocytes in the hyppocampus of patients with temporal lobe epilepsy display changes in potassium conductances. Eur J Neurosci 12:2087–2096.

Kimelberg HK, Kettenmann H. 1990. Swelling-induced changes in electrophysiological properties of cultured astrocytes and oligodendrocytes. I. Effects on membrane potentials, input impedance and cell–cell coupling. Brain Res 529:255–261.

Kimelberg HK, O'Connor ER. 1988. Swelling-induced depolarization of astrocyte potentials. Glia 1:219–224.

Kimelberg HK, Anderson E, Kettenmann H. 1990. Swelling-induced changes in electrophysiological properties of cultured astrocytes and oligodendrocytes. II. Whole-cell currents. Brain Res 529:262–268.

Krizaj D, Rice ME, Wardle RA, Nicholson C. 1996. Water compartmentalization and extracellular tortuosity after osmotic changes in cerebellum of *Trachemys scripta*. J Physiol (London) 492:887–896.

Kuffler SW, Nicholls JG, Orkand RK. 1966. Physiological properties of glial cells in the central nervous system of amphibia. J Neurophysiol 29:768–787.

Margolis RU, Margolis RK. 1974. Distribution and metabolism of mucopolysaccharides and glycoproteins in neuronal perikarya, astrocytes, and oligodendroglia. Biochemistry 13:2849–2852.

McManus ML, Strange K. 1993. Acute volume regulation of brain cells in response to hypertonic challenge. Anesthesiology 78:1132–1173.

Nicholson C, Phillips JM. 1981. Ion diffusion modified by tortuosity and volume fraction in the extracellular microenvironment of the rat cerebellum. J Physiol (Lond) 321:225–257.

Nicholson C, Syková E. 1998. Extracellular space structure revealed by diffusion analysis. Trends Neurosci 21:207–215.

Olson JE, Li G-Z. 1997. Increased potassium, chloride, and taurine conductances in astrocytes during hypoosmotic swelling. Glia 20:254–261.

Pastor A, Chvátal A, Syková E, Kettenmann H. 1995. Glycine- and GABA-activated currents in identified glial cells of the developing rat spinal cord slice. Eur J Neurosci 7:1188–1198.

Pastor A, Kremer M, Möller T, Kettenmann H, Dermietzel R. 1998. Dye coupling between spinal cord oligodendrocytes: differences in coupling efficiency between gray and white matter. Glia 24:108–120.

Pérez-Pinzon MA, Tao L, Nicholson C. 1995. Extracellular potassium, volume fraction, and tortuosity in rat hippocampal CA1, CA3 and cortical slices during ischemia. J Neurophysiol 74:565–573.

Prokopová-Kubinová Š, Syková E. 2000. Extracellular diffusion parameters in spinal cord and filum terminale of the frog. J Neurosci Res 62:530–538.

Sontheimer H, Trotter J, Schachner M, Kettenmann H. 1989. Channel expression correlates with differentiation stage during the development of oligodendrocytes from their precursor cells in culture. Neuron 2:1135–1145.

Steinhäuser C, Berger T, Frotscher M, Kettenmann H. 1992. Heterogeneity in the membrane current pattern of identified glial cells in the hippocampal slice. Eur J Neurosci 4:472–484.

Syková E. 1992. Ionic and volume changes in the microenvironment of nerve and receptor cells. In: Ottoson D, editor. Progress in sensory physiology. Berlin, Heidelberg, New York: Springer-Verlag. p 1–167.

Syková E. 1997. The extracellular space in the CNS: its regulation, volume and geometry in normal and pathological neuronal function. Neuroscientist 3:28–41.

Syková E. Chvátal A. 2000. Glial cells and volume transmission in the CNS. Neurochem Int 36:397–409.

Syková E, Svoboda J, Polák J, Chvátal A. 1994. Extracellular volume fraction and diffusion characteristics during progressive ischemia and terminal anoxia in the spinal cord of the rat. J Cereb Blood Flow Metab 14:301–311.

Syková E, Vargová L, Prokopová Š, Šimonová Z. 1999. Glial swelling and astrogliosis produce diffusion barriers in the rat spinal cord. Glia 25:56–70.

Syková E, Mazel T, Vargová L, Vořišek I, Prokopová Š. 2000. Extracellular space diffusion and pathological states. Progr Brain Res 125:155–178.

Tomita M, Fukuuchi Y, Terakawa S. 1994. Differential behavior of glial and neuronal cells exposed to hypotonic solution. Acta Neurochir 60: 31–33.

Žiak D, Chvátal A, Syková E. 1998. Glutamate-, kainate- and NMDA-evoked membrane currents in identified glial cells in rat spinal cord slice. Physiol Res 47:365–375.

Zoli M, Jansson A, Syková E, Agnati LF, Fuxe K. 1999. Volume transmission in the CNS and its relevance for neuropsychopharmacology. Trends Pharmacol Sci 20:142–150.